Abstract

This work aims to develop a stereoselective enzymatic alternative for the radiosynthesis of [^{11}C]*(S,S)*-S-adenosylmethionine ([^{11}C](*S,S*)-SAM), a potential PET-CT radiotracer for monitoring particularly aggressive prostate tumors. Conventional synthesis of this compound has been carried out at Uruguayan Center of Molecular Imaging, resulting in an almost racemic mixture 53:47 ratio of *(R,S)* to *(S,S)* isomer. Producing the radiotracer in an optically pure form is a requirement for administration to humans and additionally it would enhance diagnostic sensitivity when administered to the patient.

The main challenges were designing a biocatalyst capable of withstanding the harsh conditions of the radiotracer synthesis module and achieving the reaction in a very short time due to the rapid decay of ^{11}C.

A mutant of *E. coli* methionine adenosyltransferase (I303V MAT) with enhanced SAM synthesis was cloned, expressed, and immobilized on agarose using an irreversible covalent isourea bond. This immobilized enzyme synthesized [^{11}C](S,S)-SAM from [^{11}C]L-methionine in an automated module, with the labeled methionine produced in situ from [^{11}C]CH3I and L-homocysteine thiolactone. The product was obtained with an enantio and diasteromeric excess greater than 99% and average conversion of 80%. The reuse of the immobilized enzyme was studied, showing that after three cycles of reuse the radiosynthesis performance remained unchanged.

Keywords: enzymatic radiosynthesis; SAM; S-adenosylmethionine; methionine adenosyltransferase; immobilized enzyme; prostate cancer radiotracer, stereospecificity

1. Introduction

Biocatalysis and enzyme immobilization applied to radiochemistry

The application of biocatalysis in radiochemistry could lead to substantial improvements in synthetic efficiency and the stereochemical purity of final products. Thus, there is evidence supporting the feasibility of using enzymes in radiosynthesis [1,2]. Focusing on ^{11}C radiochemistry there is some background of biocatalytic applications in the radiosynthesis of amino acids and other small molecules, employing both soluble and immobilized enzymes that accept [^{11}C]D,L-alanine and [^{11}C]L-methionine as precursors, whose traditional synthesis from [^{11}C]CH_3I is well established [1,3,4]. However, as reviewed by Da Silva *et al.* in 2018 [1] last significant research on biocatalytic approaches based on [^{11}C]CH_3I derivates was published in the final decade of the 20th century; to the best of our knowledge, and based on global reviews of advances in ^{11}C radiochemistry, this area remains unexplored in recent years [5,6].

A plausible explanation for the limited exploration of this area could be concerns regarding potential contamination of the final product with immunogenic proteins, as well as the associated costs of obtaining active enzymatic extracts and the lack of automated technologies, whose development has facilitated the clinical application of PET tracers [7]. Nevertheless, considering the significant technological advances in the production and application of recombinant enzymes to drug synthesis over the past 30 years [8] these challenges are now more manageable.

As noted before, when developing a process for injectable drugs, the presence of

soluble proteins could pose a risk of pyrogenic contamination, a critical consideration in radiotracer production, where the final formulation must meet stringent quality standards for intravenous administration [2]. In this context, one strategy to minimize risk could involve immobilizing enzymes onto solid supports through covalent and irreversible bonds, preventing the release of proteins into the reaction media and potentially enabling the integration of enzymes into continuous flow reactions [2,9-12].

SAM and its potential as a prostate cancer radiotracer

The *(S,S)* isomer of SAM is associated with several pathophysiological alterations present in prostate cancer. For instance, it has been reported that the level of sarcosine, an intermediate and by-product in the synthesis and degradation of glycine, is elevated in the context of aggressive prostate cancers. This increase, which is associated with increased proliferation of tumor cells *in vitro*, may be related to elevated levels of the enzyme glycine N-methyltransferase (GNMT) involved in its synthesis. The concentration of GNMT is elevated in tumors with a high Gleason score and is associated with increased aggressiveness [13-16].

Considering the role of GNMT and sarcosine in the progression and aggressiveness of prostate cancer, our research group has previously postulated that the identification of potential ligands for GNMT and related metabolic intermediates for subsequent labeling with PET radionuclides would constitute a novel tool for the diagnosis of this pathology through molecular imaging with PET. In particular, focus has been placed on the *(S,S)* isomer of SAM, as it is the natural cofactor of

GNMT and therefore has the potential to serve as a good indicator of an imbalance in the enzyme's expression or activity [15]. The research team from the Radiopharmacy Department at the Uruguayan Center for Molecular Imaging (CUDIM) has faced the challenge of developing efficient local production processes for radiotracers labeled with ^{11}C for PET imaging, that meet the required quality standards according to specifications established in the USP or EP monographs. Additionally, CUDIM has developed its own synthetic processes for the different molecules used, as it is necessary to have the appropriate precursor with a reactive center for selective substitution or addition of the positron-emitting radionuclide [7,17-19]. The availability and quality of the precursor are essential for the subsequent labeling of the molecule to be injected into the patient or experimental animal. In the case of [^{11}C]SAM, the CUDIM research team has developed an automated synthesis process that generates the desired radiopharmaceutical in a racemic mixture (53:47 ratio of *(R,S)* isomer to *(S,S)* isomer) by methylation of S-adenosylhomocysteine with [^{11}C]CH_3I [15]. Despite the success of this synthesis, the lack of optical purity precluded to proceed to clinical trials in humans.

Biocatalysis could provide a solution to this problem, actually, there is one report for the biocatalytic radiosynthesis of [^{11}C]S-adenosyl-L-methionine, an enzymatic approach had been performed using [^{11}C]L-methionine and ATP with a crude extract of rat liver naturally expressing methionine adenosyltransferase (MAT) [20].

With the currently available technologies several expression systems for recombinant MAT have been developed, resulting in soluble and active enzyme in

most cases [21-26]. Of particular interest is the work reported by Niu *et al*., regarding the cloning and expression of the mutant of the *E. coli* native enzyme, reported as a variant with lower product inhibition [27].

Based on these precedents, our work focused on the development of an immobilized biocatalyst of the I303V mutant of *E. coli* MAT to perform the radiosynthesis of [^{11}C]SAM in the automated synthesis module (TracerLab FXC-Pro, GE), starting from [^{11}C]L-methionine and ATP, in the shortest possible time to avoid yield loss due to product radiochemical decay.

2. Materials and methods

2.1. Vectors, strains and culture media

The strains employed in this study were *E. coli* TOP10 obtained from Invitrogen and *E. coli* BL21(DE3) obtained from NE Biolabs. The vector utilized was pET28a(+) from Novagen, and the pET28a(+)-MAT (Genscript) vector. Standard microbiological techniques were employed for the handling of all strains. Luria-Bertani (LB) agar and liquid media, L-Broth media, as well as a previously reported Autoinduction Medium (AIM)[28], supplemented with the appropriate antibiotic when necessary (Kanamycin 50 μg/mL), were utilized for the growth of the *E. coli* strains. For further details, please refer to supplementary information.

2.2. Cloning of I303V MAT

In order to clone I303V MAT gene, the synthesis of an expression vector based on pET28a+ was entrusted to the company GenScript (This construction is the same reported by Niu *et al*)[27]. Subsequently, the cloning process was performed utilizing

in-house prepared electrocompetent cells of *E. coli* TOP10 and *E. coli* BL21(DE3). The production of electrocompetent cells and their transformation was performed following the protocol provided by Bio-Rad, with slight modifications (further details in supplementary information). The resulting clone *E. coli* BL21(DE3) (pET28a-I303V MAT) was kept as a frozen stock in 15 % glycerol, - 70 °C.

2.3. Production and purification of I303V MAT

The production of the I303V MAT enzyme was carried out using the developed strain through a classical protocol involving strain growth, cell lysis, and affinity chromatography purification.

Fresh LB-Kan plates were streaked from the frozen *E. coli* BL21(DE3) (pET28a_I303VMAT) stock, and a single colony was used to inoculate 5 mL of LB-Kan. The culture was incubated in a rotary shaker overnight (150 rpm, 37 °C), and 1 mL of this culture was used to inoculate 100 mL of fresh AIM-Kan in a 500 mL Erlenmeyer flask. The fresh culture was grown under the same conditions until it reached an OD_{600} of 0.5 (approximately 2.5 h), then the temperature was lowered to 28 °C and the culture was incubated overnight. The grown culture was centrifuged at 4000 rpm, 10 minutes, 4 °C, and resuspended in 20 mM phosphate buffer, pH 7.6, 500 mM NaCl. Lysozyme was added to a final concentration of 2 mg/mL and incubated at 28 °C for 30 minutes with slight shaking. Following this incubation, Triton X-100 (final concentration 1 %), DNase 10 μg/mL and RNase 10 μg/mL were added, and the mixture was incubated for 30 minutes under the same conditions. The lysed cells were centrifuged at 10000 rpm, 30 minutes, 4 °C to separate the cell

debris. The soluble proteins were applied to a HiTrap Chelating HP column and the protein was purified following a classical procedure. After washing with 10 mL of 20 mM phosphate sodium buffer, supplemented with 500 mM NaCl and 50 mM imidazole, pH 7.6, the protein was eluted with 15 mL of the same buffer supplemented with 500 mM imidazole. The eluted fraction was dialyzed and protein concentration was determined by the Bradford Method [29].

2.4. Enzymatic activity assay for soluble I303V MAT.

The activity was assayed at 37 °C using ATP and L-methionine as substrates.

The following reaction mixture was prepared: 148 μL of 100 mM Tris-HCl buffer pH 8.0 supplemented with 50 mM K_2SO_4 and 20 mM $MgSO_4$ (Activity buffer)[27]; 7 μL of 300 mM ATP (final concentration in the assay 10 mM); 10 μL of 200 mM L-methionine (final concentration in the assay 10 mM). The mixture was preincubated at 37 °C. A 35 μL aliquot of a suitable enzyme solution, preincubated at the same temperature, was added to the mixture. After 5 minutes, the reaction was stopped by the addition of 100 μL of 1.0 M HCl. The amount of SAM product obtained was determined using HPLC (Nucleodur ec C18 column, mobile phase: 50 mM ammonium acetate buffer with 1% TFA pH 5.4, flow rate 1 mL/min). The produced SAM was quantified by comparison with a calibration curve constructed from a commercial SAM standard (Sigma-Aldrich A7007).

The enzyme unit was defined as the amount of enzyme required to produce 1 μmol of SAM per minute under the aforementioned conditions. All assays were performed in triplicate.

158 **2.5. pH stability assay of soluble I303V MAT**

159 pH stability was studied by incubating samples of the enzyme in 10mM ATB (acetic
160 acid - Tris - boric acid) buffer at four different pH (5, 7, 9, and 11) at room
161 temperature. Samples were collected at different time points over a 24-hour period
162 to assess the enzymatic activity. The remaining activity for each sample was
163 calculated as a percentage relative to the activity recorded at the initial time point
164 (considered as 100% activity). All assays were performed in triplicate.

165 **2.6. Immobilization of I303V MAT in CDAP- Sepharose**

166 Agarose (Sepharose™ 4B) was activated with 1-Cyano-4-Dimethylaminopyridine
167 Tetrafluoroborate (CDAP) according to Giacomini *et al*.[30].

168 Covalent immobilization of the enzyme was carried out by incubation of 1 g of
169 suction dried activated carrier, with purified enzyme solution in 1:8 w/v ratio. The
170 suspension was gently agitated at room temperature for 4 h. The immobilized
171 enzyme was exhaustively washed with Tris-HCl 100mM pH 8.0 buffer, then
172 equilibrated with the activity buffer and stored at 4 °C until use.

173 **2.7. Enzymatic activity assay for the immobilized I303V MAT**

174 The following reaction mixture was prepared: 358 μL of activity buffer, 17 μL of 300
175 mM ATP (10 mM final concentration in the assay), and 25 μL of 200 mM L-
176 methionine (10 mM final concentration in the assay). The mixture was preincubated
177 at 37 °C. A standard suspension was prepared with 100 mg of suction dried I303V
178 MAT-CDAP-agarose derivative in 1mL of activity buffer and preincubated at 37 °C.
179 Subsequently, 100 μL of the standard suspension was added to the mix solution and

incubated with agitation at 37 °C. After 7 minutes, the reaction was stopped by adding 250 µL of 1M HCl. The samples were then centrifuged, and the supernatant was filtered using a 0.22 µm filter. The amount of SAM product obtained was determined using HPLC as described in 2.4. All activity assays were performed in triplicate.

2.8. Production of [^{11}C]CH_3I

The radioactive precursor [^{11}C]CH_3I was produced into an automatized module (General Electric TRACERlab® FX C Pro), according to the method described by Buccino *et al*. and Zoppolo *et al*. starting from [^{11}C]CO_2 produced in a PET Trace® 16.5 MeV cyclotron (GE Healthcare) [7,15].

2.9. Enzymatic radiosynthesis of [^{11}C](*S,S*)-SAM from [^{11}C]L-methionine with I303V MAT-CDAP-agarose derivative

All radiosynthesis were performed into the automatized module TRACERlab® FX C Pro, with the necessary adaptations to perform enzymatic reactions.

The generated [^{11}C]CH_3I was passed through a Sep-Pak C18 Plus Light column to react with L-homocysteine thiolactone, producing [^{11}C]L-methionine. Afterwards, the generated [^{11}C]L-methionine was eluted into the collection flask using the activity buffer from vial 3 (V3 in Figure S1 in supplementary information). When the [^{11}C]L-methionine reached the collection flask, the enzymatic reaction took place. Magnetic stirring was employed to facilitate the interaction between the immobilized enzyme derivative and the substrates. Enzymatic synthesis times of 5 and 10 minutes were tested. After the designated time, the content of the collection

flask was transferred to the final vial using helium flow, passing through a filter to retain the insoluble enzymatic derivative. To analyze the result of the radiosynthesis, the final vial was removed from the automated module and the final radioactivity of the synthesis was measured. The obtained products were immediately analyzed by HPLC (Nucleodur ec C18 column, mobile phase: 50 mM ammonium acetate buffer with 1% TFA at pH 5.4, flow rate 1 mL/min, UV and Gamma detectors). These conditions ensure clear separation of the SAM diastereomers. Peaks were assigned through comparison with L-methionine and SAM true standard (Sigma Aldrich A7007) as previously reported by Zoppolo *et al.* [15]. Conversion was calculated as the area ratio between the SAM peak compared to the added SAM and L-methionine peaks, based on the gamma signal in the HPLC chromatogram.

2.10. Purification of [^{11}C](*S,S*)-SAM from the reaction mixture

The reaction mixture from the collection flask was purified by solid phase extraction (SPE) method. The reaction mixture was diluted by the addition of water for injection (15 mL) from vial 2(V2), and subsequently transferred through a Strata XC-SPE cartridge (Phenomenex) (pre-activated with 1 mL of absolute ethanol followed by 1 mL of 0.1 M sodium acetate buffer pH 4.5). The cartridge was washed with 10 mL of 0.1M HCl from vial 4 (V4) and 15 mL of water for injection from vial 5 (V5). The trapped product was eluted with 4 mL of Na_2HPO_4 0.1 M pH 8.5: EtOH (9:1) from vial 6 (V6). The final solution was transferred through a Sep-Pak tC18 Plus Short cartridge (Waters) (pre-activated with 5 mL of absolute ethanol followed by 10

mL of water for injection). Note: for further information about vial ubication in module, please refer to Figure S1 in supplementary information.

3. Results and Discussion

3.1. Production and purification of I303V MAT

As already mentioned, the I303V mutant of the *E. coli* MAT enzyme was selected as candidate for the synthesis of SAM since it presents lower product inhibition than the wild-type enzyme [27]. Electrocompetent cells of *E. coli* BL21(DE3) were transformed with the pET28a_I303VMAT vector, yielding the desired expression strain, *E. coli* BL21(DE3) (pET28a_I303VMAT). To optimize I303V MAT expression, variations in the growth temperature of the cells (30 and 37 °C), protein expression incubation temperature (30 and 28 °C), culture medium (LB-Kan and AIM-Kan) and induction condition (IPTG and lactose autoinduction) were tested. All combinations studied yielded a large amount of enzyme expressed in soluble form (for further information, please refer to the supplementary information Figure S2 and Table S1). The selected conditions were 37 °C as the growing temperature and 28 °C for protein expression in an autoinduction medium that offers the additional advantage of avoiding the need for the IPTG inducer, making it a more cost-effective option.

To facilitate the purification, the enzyme was expressed with a polyhistidine-tag at the N-terminal end, so a classic purification protocol via IMAC was implemented (the purification process was followed by SDS PAGE, available in Figure S3 in supplementary information). The final purification yield was 155 mg of protein per

liter of culture, surpassing the yield reported by Niu *et al*. for I303V MAT (100 mg/L) [27]. In terms of enzyme activity, the process was highly efficient recovering 100% of the initially applied activity; the purified enzyme solution showed an enzyme activity of (4.0 ± 0.2) U/mL and a specific activity of (0.65 ± 0.07) U/mg of protein. Considering specific activity data, the obtained enzyme was 7-fold purer than the initial lysate (Table S2 in supplementary information).

3.2. I303V MAT stability studies with pH

To select the appropriate immobilization method, pH stability studies were conducted, and the results are illustrated in Figure 1. The studies were performed at room temperature. In accordance with the literature, the enzyme was completely inactive at pH 5.0 under the incubation conditions, independently of the incubation time [27]. Furthermore, at neutral and alkaline pH (7.0 and 9.0) the enzyme remained stable for 24-hour at room temperature, retaining over 90% of the initial enzyme activity. Concerning pH 11.0, although there was loss of activity over the course of the incubation time, it still conserved over 80% of the initial enzyme activity after 20 hours. These results indicated that the produced enzyme could be subject of immobilization strategies that requires incubation at neutral to moderate alkaline pH, without compromising its activity.

3.3. Immobilization of I303V MAT in agarose activated with CDAP

As previously mentioned, considering the process characteristics and the intended purpose, the implementation of an insoluble immobilized enzyme derivative would diminish the chance of enzyme presence in the final product, avoiding additional

266 purification steps, which are time consuming and its implementation in the
267 automated synthesis module would be challenging.
268 Therefore, in order to minimize protein leakage during the radiotracer synthesis, a
269 strategy of covalent immobilization between the enzyme and the solid support was
270 chosen. In this regard, CDAP-activated agarose was selected as the support; it
271 contains reactive cyanate ester groups on its surface, allowing the formation of
272 covalent isourea-type bonds through reaction with amino groups of the protein,
273 under mild reaction conditions. With the aim of identifying surface lysine residues
274 that could provide potential amino groups for immobilization onto the chosen
275 support, a study was conducted using the previously reported crystal structure of
276 the MAT enzyme [31] and Pymol [32]. The confirmation of an adequate quantity of
277 surface ε-amino groups from lysine residues, in addition to the N-terminal amino
278 group, was established (see supplementary data Figure S4). Upon the application of
279 I303V MAT (51.2 ± 5.7 mg of protein containing 32.5 ± 0.9 U/g of suction dried gel)
280 on CDAP-agarose, 36.4 ± 5.8 mg of protein corresponding to 71% of the applied
281 amount of protein and 17.0 ± 1.0 U corresponding to 39 % of the applied enzyme
282 activity was immobilized. These results were calculated by the difference between
283 the amount of protein or activity applied and the amount of protein or enzyme
284 activity in the supernatant and washing fractions. The coupling efficiency, calculated
285 as the percentage of the expressed activity relative to the immobilized one, was
286 100%, indicating that all the enzyme bound to the support remained active.
287 Niu *et al*. [27] reported the immobilization of the I303V MAT on an amino resin (LX-

1000HA) derivatized with glutaraldehyde, through the formation of a Schiff base between the ε-amino groups of lysine and the aldehyde on the support. The major difference between Niu's immobilized enzymatic derivative and the one constructed in this work is the binding chemistry: while the approach reported by Niu *et al.* is based on the formation of a reversible Schiff base, the CDAP strategy employed herein involves the formation of a covalent and irreversible isourea bond, preventing enzyme release from the support, which is highly desirable for the intended application. Given the immobilization pH of 7.0, the N-terminal amino group of the protein exhibits the highest reactivity, making it the probable initial anchoring point between the protein and the support. The inclusion of the N-terminal histidine tag may introduce some flexibility to the structure, enabling subsequent multi-point attachment by promoting the reaction through the less reactive ε-amino groups of lysine residues. This would be favorable for the integrity of the immobilized derivative.

Thus, the I303V MAT-CDAP-agarose derivative obtained was considered a very suitable candidate for use in the radiotracer synthesis.

3.4. Kinetic parameters of soluble and immobilized enzyme

It is well-known that immobilization to solid supports generally affects the kinetic parameters of the enzymes. This reflects either conformational changes that affect the affinity of the enzyme for the substrates and/or the existence of diffusional restrictions due to immobilization. The results in Table 1 show that the Km values for ATP and L-methionine were of the same order for both, the soluble and

immobilized enzymes, and that the turnover numbers (Kcat values) were also comparable. These results suggest that the immobilization process employed had a negligible impact on the enzyme's performance, which highlights an additional advantage of the chosen immobilization method.

3.5. Determining the enantio and diastereoselectivity of I303V MAT for the proposed synthesis

For the intended purpose, the molecule selected as radiotracer is the biologically active isomer of SAM: (*S*,*S*)-S-adenosylmethionine. Although wild type MAT is known to provide only one diastereomer in nature; the stereoselectivity of the I303V MAT mutant has not been established and mutations can affect enzyme parameters. Diastereoselectivity of the enzyme was proven by HPLC comparison of the product with a true standard containing both diastereomers (Figure 4). Regarding enantioselectivity, the major issue was associated with the fact that [^{11}C]methionine was produced as a 90:10 mixture of [^{11}C]L-methionine:[^{11}C]D-methionine, which could potentially lead to the formation of other diastereomers of SAM if the enzyme was capable of accepting D-methionine as a substrate. To verify that the (*S*,*S*)-S-adenosylmethionine diastereomer was the major outcome in enzymatic radiosynthesis, the rates of SAM formation from D-methionine or L-methionine and ATP were evaluated. For D-methionine, reaction progress at 30, 45, 60, 75, and 90 minutes was assessed. The results indicate that within the studied time, the reaction was operating under initial rate conditions (see Figure 2), an essential feature for data comparison. The catalytic rate for the conversion of L-methionine was (1.7 ± 0.1)

U/mL, while for D-methionine it was (0.06 ± 0.01) U/mL. This indicates that the enzyme was 23 times more efficient at converting L-methionine compared to its isomer, D-methionine. This kinetic difference, along with the fact that, [^{11}C]methionine radiosynthesis yields the L-isomer in a 90:10 ratio, indicate that the production of *(R,R)*-SAM isomer in the radiosynthesis conditions is neglectable.

3.6. Enzymatic radiosynthesis of [^{11}C](*S,S*)-SAM from [^{11}C]L-methionine using the I303V MAT-CDAP-agarose derivative

The radiosynthesis was carried out in the GE Tracerlab FXC-Pro automated module, following the procedure described in section 2.9, employing the enzymatic immobilized derivative in suspension in the reaction mixture with mild magnetic stirring, in order to avoid diffusional problems and promote catalysis. After completion of the synthesis, the immobilized derivative was separated from the final product by filtration with a column frit (pore size 20-85 Å). The inclusion of this filter implied a modification of the automated module TracerLab FXC-Pro. The final configuration of the system is shown in Figure 3.

Different combination of reaction time and enzyme units were tested, and the major results are summarized in Table 2. Conversion was calculated as the area ratio between the SAM peak compared to the added SAM and L-methionine peaks, based on the gamma signal in the HPLC chromatograms, (Figure 4). A conversion of (87.3 ± 1.8)% (n=3) was achieved using a enzymatic activity of 18.2 U in the reaction mixture and 10 minutes reaction time (Table 2). Under these conditions, a diastereomeric excess of over 99% was determined, demonstrating that radioactivity

did not alter the enzyme's stereoselectivity. As mentioned earlier, the previously reported synthesis yielded a ratio of isomers (*R*,*S*):(*S*,*S*) at 53:47 [15], thus, the enzymatic method represents a superior option in terms of optical purity of the product. As an example, Figure 4 presents a chromatogram of the reaction mixture achieved after 10 min catalyzed by the immobilized enzyme (Table 2, row 1), registered by UV and gamma detectors. The observed peak profile was consistent across all tested conditions.

To evaluate the overall radiochemical yield, which indicates how much of the produced [^{11}C]CH_3I was converted to [^{11}C]SAM, the total radioactivity of the crude at the end of the synthesis was considered. Using the HPLC chromatogram, it was possible to assign how much of this radioactivity corresponded to [^{11}C]SAM. The ratio of this calculated value to the initial radioactivity of [^{11}C]CH_3I, measured before [^{11}C]methionine synthesis, is reported as the radiochemical yield, with non-decay correction (ndc). Figure 5, columns 2 and 3, show that the radiochemical yield obtained with the immobilized enzyme at 10 and 5 minutes of reaction, compared to the previously reported procedure (column 1)[15] are comparable. However, the enzymatic synthesis occurs with an enantiomeric excess greater than 99% and thus the quantity of the biologically active [^{11}C]SAM produced is almost twice that produced with the previous method.

Due to radioactive decay and considering the ^{11}C half-life of 20.4 min, minimizing the reaction time is crucial for preserving the highest possible level of radioactivity at the end of the process. Additionally, a reduction of the immobilized enzyme

quantity in the reaction mix could be favorable not only from an economic but also from a technical point of view, because manipulating smaller quantities of solid derivative would improve the post-synthesis filtration process, thereby diminishing the risk of system blockages and accelerating the process. Therefore, we assessed the impact of reducing the synthesis time from 10 to 5 minutes, and immobilized enzyme concentration to a third of the initial quantity, obtaining only a slight decrease in conversion. Therefore, the decision to reduce the synthesis time and enzyme concentration was deemed advantageous for the overall process efficiency.

Based on all the abovementioned results, the most suitable conditions for the radiosynthesis of optically pure [^{11}C]*(S,S)*-SAM were set on the immobilized enzyme with an enzymatic activity of 4.8 U in the mixture and a reaction time of 5 minutes. For the intended application, the radiochemical yields were deemed satisfactory, with the added potential for optimizing the product quantity through an increase in the initial amount of [^{11}C]CH_3I produced.

3.7. Reuse of the immobilized enzyme

Once the reaction conditions were defined, studies were initiated to determine the feasibility of reusing the immobilized biocatalyst. For this, successive experiments were carried out with the same immobilized enzyme derivative, in the selected conditions, determining the radiochemical yields (as defined in Table 2), which remained practically constant after three uses: 11.0 ± 1.2 initial vs 12.2 ± 1.1 after the third use. Further studies should be conducted to determine the maximum number of reuses that maintain an acceptable yield for the intended application, without

compromising the purity of the final product through enzyme contamination.

3.8. Radiochemical yield of the [^{11}C](S,S)-SAM purified from de reaction mixture

After selecting the optimal radiosynthesis conditions, the next step was to isolate the desired radiotracer by separating it from any other radioactive compounds in the mixture. To achieve this, a purification protocol was optimized, as detailed in section 2.10 (see Figure S5 un supplementary information). The radiochemical yield of the purified [^{11}C](S,S)-SAM, relative to the initial amount of [^{11}C]CH_3I, was (6.8 ± 1.3)%, non-decay corrected, (n=5).

The radiochemical yield of the purified radiotracer obtained enzymatically is slightly lower compared to the value previously reported by Zoppolo (2017) [15] for the classical chemical synthesis, (6.8 ± 1.3)% and (10 ± 2)%, respectively. However, it is important to highlight that, in the case of the chemical synthesis, the reported yield corresponds to a diastereomeric mixture of 53:47 [(R,S)-isomer: (S,S)-isomer]. Consequently, even if the total radiochemical yield appears similar, the enzymatic process is more efficient in delivering the biologically active product, providing a solution for the optical pure synthesis of [^{11}C](S,S)-SAM. This will allow to continue the characterization of [^{11}C]*(S,S)*-S-adenosylmethionine as a radiotracer for prostate cancer diagnosis and characterization.

4. Conclusions

The *(S,S)*-SAM is a biologically active molecule with great potential as a PET radiotracer in processes that involve the overexpression of SAM dependent methyl transferases. Diagnostic radiotracers are subjected to the same regulations than all

pharmaceuticals, including optical purity of the drug. In this sense, biocatalysis can contribute to the stereoselective synthesis of this type of compounds.

In this work, the enzymatically catalyzed radiosynthesis of [^{11}C](*S*,*S*)-SAM using an immobilized derivative of I303V MAT was achieved with an average of 80% of conversion and 6.8% radiochemical yield (ndc) of the pure radiotracer, what is slightly lower to the previously reported classical procedure. The major advantage of the enzymatic strategy described herein relates to the optical purity of the product, that was obtained with a diastereomeric excess greater than 99% with the *(S,S)* enantiomer as the major product (*ee* > 99%)**.** The adaptation of the automated radiosynthesis module for the use of the immobilized enzyme was achieved, and synthesis conditions such as enzyme load and reaction time were optimized. The use of a covalently immobilized enzyme diminishes the risk of enzyme contamination in the final product and allows reutilization of the biocatalyst, lowering the potential associated costs when compared with classical procedures. In addition, it simplifies the purification process of the labeled product, resulting in a reduction in the overall process time, a crucial fact for the success of the development.

The results of this work demonstrate that biocatalysis is an optimal choice for the development of radiosynthesis, especially when stereoselectivity in the desired product is required, and that adapting this type of synthesis to automated modules is possible, which makes the clinical application of the target radiotracer feasible.

References

[1] E.S. da Silva, V. Gómez-Vallejo, F. López-Gallego. J. Llop, Biocatalysis in radiochemistry: Enzymatic incorporation of PET radionuclides into molecules of biomedical interest. J. Label. Compd. Radiopharm. 61 (2018)332–354.

[2] M.R. Kilbourn, P. Scott. Handbook of Radiopharmaceuticals: Methodology and Applications, second ed. Wiley, 2021.

[3] B Långström, G Antoni, P Gullberg, C Halldin, P Malmborg, K Någren, A Rimland, H Svärd, Synthesis of L- and D-[Methyl-11C]Methionine. J. Nucl. Med. 28 (1987) 1037–1040.

[4] V. Pichler, C. Vraka, N. Berroterán-Infante, A. Krcal, H. Eidherr, T. Traub-Weidinger, M. Hacker, M. Mitterhauser, W. Wadsak, L-[S-methyl-11C]methionine: An example of radiosynthetic optimization. Appl. Radiat. Isot. 141 (2018) 107–111.

[5] K. Dahl, C. Halldin, M. Schou, New methodologies for the preparation of carbon-11 labeled radiopharmaceuticals Clin Transl Imaging. 5 (2017) 275-289. OI: 10.1007/s40336-017-0223-1

[6] J. Rong, A. Haider,T.E. Jeppesen, L. Josephson, S.H. Liang, Radiochemistry for positron emission tomography. Nat. Commun. 14 (2023) 3257.

[7] P. Buccino, I. Kreimerman, K. Zirbesegger, W. Porcal, E. Savio, H. Engler, Automated radiosynthesis of [11 C]L-deprenyl-D 2 and [11 C]D-deprenyl using a commercial platform. Appl. Radiat. Isot.110 (2016) 47-52 https://doi.org/10.1016/j.apradiso.2015.12.051

[8] Patel, R. N. Biocatalysis for synthesis of pharmaceuticals. Bioorg. Med. Chem. 26 (2018) 1252–1274.

462 [9] B. Brena, P. González-Pombo, F. Batista-Viera, Immobilization of enzymes: A literature
463 survey. Methods Mol. Biol. 1051 (2013) 15–31.
464 [10] H-J. Federsel, T.S. Moody, S. J.C. Taylor, Recent Trends in Enzyme Immobilization-
465 Concepts for Expanding the Biocatalysis Toolbox. Molecules 26 (2021)
466 doi:10.3390/molecules26092822.
467 [11]J.M. Guisan, New opportunities for immobilization of enzymes. Methods Mol. Biol.1051,
468 (2013)1–13. doi: 10.1007/978-1-62703-550-7_1
469 [12]R.C. Rodrigues, A. Berenguer-Murcia, D. Carballares, R. Morellon-Sterling, R.
470 Fernandez-Lafuente, Stabilization of enzymes via immobilization: Multipoint covalent
471 attachment and other stabilization strategies. Biotechnol. Adv. 52, (2021). doi:
472 10.1016/j.biotechadv.2021.107821.
473 [13]F. Giunchi, M. Fiorentino, M. Loda, The Metabolic Landscape of Prostate Cancer. Eur.
474 Urol. Oncol. 2 (2019) 28–36. DOI: 10.1016/j.euo.2018.06.010
475 [14] A.P. Khan , T.M. Rajendiran, B. Ateeq, I.A. Asangani, J.N. Athanikar, A.K. Yocum, R.
476 Mehra, J. Siddiqui, G. Palapattu, J.T. Wei, G. Michailidis, A. Sreekumar, A. M. Chinnaiyan,
477 The role of sarcosine metabolism in prostate cancer progression. Neoplasia. 15, (2013) 491–
478 501. DOI: 10.1593/neo.13314
479 [15]F. Zoppolo, W. Porcal, P. Oliver, E. Savio, H. Engler, Automated One-pot Radiosynthesis
480 of [11C]S-adenosyl Methionine. Curr. Radiopharm. 10 (2017) 203–211.
481 doi: 10.2174/1874471010666170718171441
482 [16]D.F. Gleason, Classification of prostatic carcinomas. Cancer Chemother. Rep. 50 (1966)
483 125–128.

[17] P. Buccino, I. Kreimerman, E. Savio, H. Engler, Synthesis and quality control of [^{11}C]Deuterodeprenyl using the automated module General Electric (GE) TRACERlab® FX C Pro. Journal of Nuclear Medicine . 55 (2014) supplement 1, 1251.

[18] K. Zirbesegger, P. Buccino, I. Kreimerman, H. Engler , W. Porcal, E. Savio, An efficient preparation of labelling precursor of [11C]L-deprenyl-D2 and automated radiosynthesis. EJNMMI Radiopharm. Chem. 2 (2017). https://doi.org/10.1186/s41181-017-0029-5

[19] S. Rivera-Marrero, A. Bencomo-Martínez, E. Orta Salazar, M. Sablón-Carrazana, L. García-Pupo, F. Zoppolo, F. Arredondo, R. Dapueto, M.D. Santi, I. Kreimerman, T. Pardo, L. Reyes, L. Galán, S. León-Chaviano, L.A. Espinosa-Rodríguez, R. Menéndez-Soto Del Valle, E. Savio, S. Díaz Cintra, C.Rodríguez-Tanty, A new naphthalene derivative with anti-amyloidogenic activity as potential therapeutic agent for Alzheimer's disease. Bioorg. Med. Chem. 28 (2020)115700. DOI: 10.1016/j.bmc.2020.115700

[20] K. Ishiwata, T. Ido, H. Sato, R. Iwata, K. Kawashima, K. Yanai, S. Watanuki, H. Ohtomo, K. Kogure, Simplified enzymatic synthesis and biodistribution of 11C-S-adenosyl-l-methionine. Eur. J. Nucl. Med. 11 (1986)449–452. DOI: 10.1007/BF00261008

[21] H. Chen, Z. Wang, H. Cai, C. Zhou, Progress in the microbial production of S-adenosyl-l-methionine. World J. Microbiol. Biotechnol. 32 (2016)1–8. DOI: 10.1007/s11274-016-2102-8

[22] E.S. Choi, B.S. Park, S.W. Lee, M.K. Oh, Increased production of S-adenosyl-L-methionine using recombinant Saccharomyces cerevisiae sake K6. Korean J. Chem. Eng. 26 (2009) 156–159. https://doi.org/10.1007/s11814-009-0025-x

505 [23]J. Chu, J. Qian, Y. Zhuang, S. Zhang, Y. Li, Progress in the research of S-adenosyl-l-
506 methionine production. Appl. Microbiol. Biotechnol. 97 (2013) 41–49. DOI:
507 10.1007/s00253-012-4536-8
508 [24] J.Park, J. Tai, C.A. Roessner, A.I. Scott, Enzymatic synthesis of S-adenosyl-L-methionine
509 on the preparative scale. Bioorg. Med. Chem. 4 (1996) 2179–2185. DOI: 10.1016/s0968-
510 0896(96)00228-3
511 [25] P. Yu, P. Zhu, Improving the production of S -adenosyl- L-methionine in Escherichia
512 coli by overexpressing metk. Prep. Biochem. Biotechnol. 47 (2017) 867–873.
513 https://doi.org/10.1080/10826068.2017.1350976
514 [26]P. Yu, X. Shen, Enhancing the production of S-adenosyl-Lmethionine in Pichia pastoris
515 GS115 by metabolic engineering. AMB Express 2 (2012) 1–7. doi/10.1186/2191-0855-2-57
516 [27]Niu, W., Cao, S., Yang, M. & Xu, L. Enzymatic Synthesis of S-Adenosylmethionine Using
517 Immobilized Methionine Adenosyltransferase Variants on the 50-mM Scale. Catalysts 7,
518 238 (2017). https://doi.org/10.3390/catal7080238
519 [28] N. Tahara, I. Tachibana, K. Takeo, S. Yamashita, A. Shimada, M. Hashimoto, S.
520 Ohno, T. Yokogawa, T. Nakagawa, F. Suzuki, A. Ebihara, Boosting Auto-Induction of
521 Recombinant Proteins in Escherichia coli with Glucose and Lactose Additives. Protein Pept.
522 Lett. 28 (2020)1180–1190. doi: 10.2174/0929866528666210805120715
523 [29] M.M. Bradford, A rapid and sensitive method for the quantitation of microgram
524 quantities of protein utilizing the principle of protein-dye binding. Anal. Biochem. 72
525 (1976) 248–254.

526 [30]C. Giacomini, A. Villarino, L. Franco-Fraguas, F. Batista-Viera, Immobilization of β-
527 galactosidase from Kluyveromyces lactis on silica and agarose: Comparison of different
528 methods. J. Mol. Catal. - B Enzym. 4 (1998) 313–327.
529 [31]J. Komoto, T. Yamada, Y. Takata, G.D. Markham, F. Takusagawa, Crystal structure of
530 the S-adenosylmethionine synthetase ternary complex: a novel catalytic mechanism of S-
531 adenosylmethionine synthesis from ATP and Met. Biochemistry 43 (2004) 1821–1831.
532 https://doi.org/10.1021/bi035611t
533 [32] L. Schrödinger, W. DeLano, (2020). PyMOL.
534 FIGURE LEGENDS
535
536 Figure 1. pH stability studies for I303V MAT. All studies were performed at room
537 temperature.
538
539 Figure 2. Rate of SAM formation from L-methionine vs D-methionine.
540
541 Figure 3. Left: illustrative photo of the automatized module (General Electric
542 TRACERlab® FX C Pro). Right: Scheme of the automatic module configuration for
543 the synthesis using the immobilized derivative.
544
545 Figure 4. HPLC chromatogram of the radiosynthesis of [^{11}C] *(S,S)*-SAM catalyzed by
546 the immobilized enzyme, 10 min reaction synthesis, 18.2 U of enzymatic activity.
547 Green: reaction crude, gamma detector. Red: reaction crude, UV detector λ = 254 nm.

548 Blue: SAM standard (diasteromeric mixture), UV detector λ = 254 nm. **1**: [^{11}C]L-

549 methionine, **2**: [^{11}C]*(S,S)*-SAM, **3**: *(R,S)*-SAM.

550

551 Figure 5. Radiochemical yield % (ndc) of [^{11}C]SAM obtained in reaction. 1: Classic

552 Synthesis; 2: Immobilized derivative, (10 min reaction); 3: Immobilized derivative (5

553 min reaction)

554

555

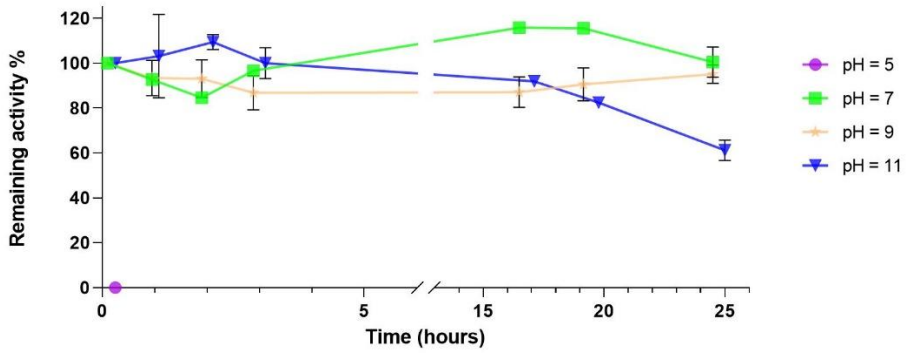

556

557

558 Figure 1

559

560

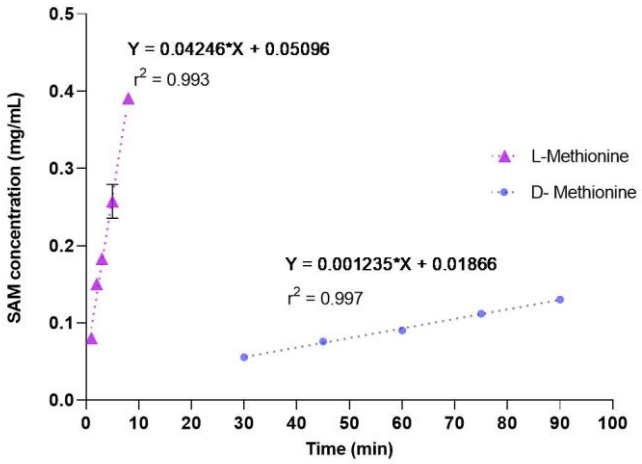

561

562 Figure 2.

563

564

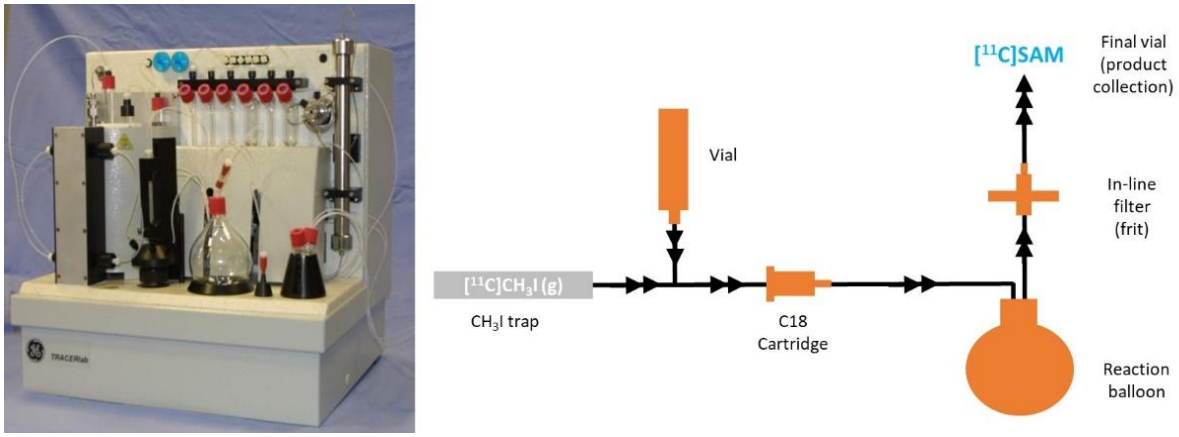

565

566 Figure 3

567

568

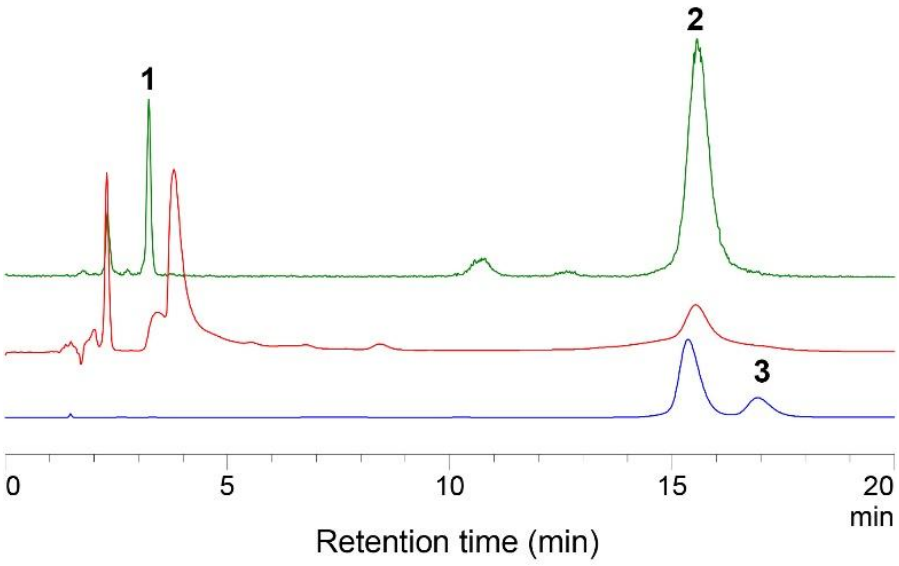

569

570

571 Figure 4

572

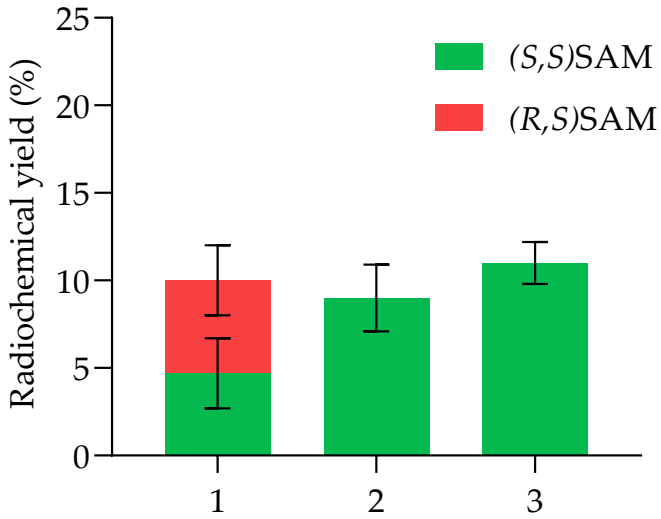

Figure 5

Enzyme I303V MAT	Km ATP (mM)	Km L-Met (mM)	Kcat (s^{-1})
Soluble	0.68 ± 0.10	1.52 ± 0.66	1.43 ± 0.06
Immobilized	0.90 ± 0.13	3.16 ± 1.26	1.37 ± 0.08

Table 1. Kinetic parameters for soluble and immobilized I303V MAT

581 Table 2. Variations in [^{11}C](*S,S*)-SAM radiosynthesis conditions using the I303V

582 MAT-CDAP-agarose derivative

Total enzymatic activity in reactive mixture (U)	**Reaction time (min)**	**% Conversion [a]**	**Radiochemical Yield (%, ndc) [b]**	**% *de* (%) [c]**
18.2	10	87.3 ± 1.8	9.1 ± 1.9	> 99
16.0	5	80*	16.5*	> 99
4.8	5	80.2 ± 9.5	11.0 ± 1.2	> 99

[a] Calculated as the area ratio between the [^{11}C]*(S,S)*-SAM peak compared to the added [^{11}C]*(S,S)*-SAM and [^{11}C]L-methionine

[b] Calculated as the relation between the radioactivity corresponding to [^{11}C]*(S,S)*-SAM in the reaction mixture and initial quantity of [^{11}C]CH_3I radioactivity, **non-decay** corrected (ndc)

[c] diastereomeric excess percentage

All experiments were performed by triplicate (n=3) with exception of the one marked*. Due to technical problems generated by applying great quantities of immobilized derivative in the automated module, it was decided not to make more replicas of this experiment and continue with lower amounts of enzyme (4.8 U, row 3), that showed comparable outcome.

583

584